Tubulin Dynamics in Cultured Mammalian Cells

WILLIAM M. SAXTON, DEREK L. STEMPLE, ROGER J. LESLIE, EDWARD D. SALMON, MICHAEL ZAVORTINK, and J. RICHARD McINTOSH
Department of Molecular, Cellular and Developmental Biology, University of Colorado at Boulder 80309

ABSTRACT Bovine neurotubulin has been labeled with dichlorotriazinyl-aminofluorescein (DTAF-tubulin) and microinjected into cultured mammalian cells strains PTK_1 and BSC. The fibrous, fluorescence patterns that developed in the microinjected cells were almost indistinguishable from the pattern of microtubules seen in the same cells by indirect immunofluorescence. DTAF-tubulin participated in the formation of all visible, microtubule-related structures at all cell cycle stages for at least 48 h after injection. Treatments of injected cells with Nocodazole or Taxol showed that DTAF-tubulin closely mimicked the behavior of endogenous tubulin. The rate at which microtubules incorporated DTAF-tubulin depended on the cell-cycle stage of the injected cell. Mitotic microtubules became fluorescent within seconds while interphase microtubules required minutes. Studies using fluorescence redistribution after photobleaching confirmed this apparent difference in tubulin dynamics between mitotic and interphase cells. The temporal patterns of redistribution included a rapid phase (~3 s) that we attribute to diffusion of free DTAF-tubulin and a second, slower phase that seems to represent the exchange of bleached DTAF-tubulin in microtubules with free, unbleached DTAF-tubulin. Mean half times of redistribution were 18-fold shorter in mitotic cells than they were in interphase cells.

The organization and apparent function of microtubules in cultured mammalian cells vary markedly as the cell cycle proceeds from interphase to mitosis and back to interphase again. Structural studies with polarization optics, immunofluorescence, and electron microscopy have shown that the mitotic spindle is an active structure in which microtubules exhibit rather rapid changes in arrangement and length (11–13, 22, 23, 27, 31, 38). The function of mitotic microtubules has been the subject of a great deal of debate for many years (reviewed in references 11 and 27), but it is clear that they are involved in the movement of chromosomes. Interphase cytoskeletal microtubules appear comparatively static with changes in arrangement and length occurring slowly (15). Although their function is also the subject of debate, they may be involved in the specification of cell polarity, shape, and cytoplasmic organization (3, 22, 28, 37, 44).

To understand the different behaviors of microtubules in mitotic and interphase cells, it may be useful to investigate the dynamic relationship between tubulin and microtubules in vivo. Studying this relationship in detail requires a method for viewing tubulin in both polymer and dimer form in living cells. In principle, microinjection of fluorescently labeled tubulin followed by fluorescence microscopy provides such a method. In practice it is a useful method only if the labeled tubulin retains the functional characteristics of the native protein (17, 18, 36, 40). Recent work supports the belief that the behavior of tubulin labeled with dichlorotriazinyl-aminofluorescein (DTAF) is analogous to the behavior of unlabeled tubulin (15, 19, 38, 39).

In this paper we report the use of DTAF-tubulin and recently developed techniques of fluorescent analogue cytochemistry (18, 30, 32, 35, reviewed in references 17, 34, 36, and 41) to study in vivo tubulin dynamics by two different methods: the rate of incorporation of DTAF-tubulin by microtubules immediately following microinjection, and the rate of fluorescence redistribution after photobleaching (FRAP) of DTAF-tubulin after the incorporation process has proceeded to steady state. Both methods indicate that the apparent rate of exchange of free tubulin dimers with tubulin dimers in polymer is rapid in mitotic microtubules relative to interphase microtubules. Our controls indicate that the presence of photobleached DTAF-tubulin and the act of photobleaching do not significantly disrupt the observed tubulin dynamics. Our results raise the possibility that underlying the differences in organization and apparent function of mitotic and interphase microtubules there is a fundamental difference in the dynamic behavior of tubulin.

MATERIALS AND METHODS

Cell Culture: Rat kangaroo cells (PTK_1) and African green monkey

THE JOURNAL OF CELL BIOLOGY · VOLUME 99 December 1984 2175-2186

kidney cells (BSC) were grown as previously described (47). PTK_1 cells were usually used to study mitotic spindles because they remain relatively flat during mitosis. BSC cells were usually used for interphase studies because their extremely flattened interphase morphology results in higher contrast microtubule images than can be obtained with interphase PTK_1 cells. Controls using PTK_1 interphase and BSC mitotic cells showed that observed tubulin dynamics are dependent on cell-cycle stage and independent of the cell type used (see Results). Cells used for electron microscopy were grown on glow discharged and ultraviolet sterilized Formvar-coated gold finder grids (Ernest F. Fullam Inc., Schenectady, NY).

Preparation of Fluorescent Proteins: DTAF-labeled bovine neurotubulin was prepared by the method of Keith et al. (15) modified as described by Leslie et al. in an accompanying paper (19). Polymerization-incompetent microtubule protein (MTP) was prepared by vacuum dialysis of the supernatant obtained from the first warm centrifugation after labeling (dialyzed against 10^4 vol of tubulin assembly buffer for 48 h at 4°C). Final protein concentration was 2.7 mg/ml. Rhodamine isothiocyanate (RITC)-labeled actin was prepared by the protocol of Wang and Taylor (42). Rhodamine- and fluorescein-labeled ovalbumin and BSA were prepared as described by Zavortink et al. (46). Fluoresceinated rabbit anti-sheep antibody (IgG fraction) was purchased from Miles Laboratories (Elkhart, IN).

Microinjection: Proteins were prepared for microinjection by dialysis against 1,000 vol of injection buffer (140 mM K^+, 100 mM Na-glutamate, 40 mM citrate, 1 mM $MgCl_2$, 1 mM EGTA, 0.1 mM GTP, at pH 7.2). This buffer was chosen because it served to stabilize the polymerization competence of the purified tubulin and was not visibly deleterious to cells when microinjected (46). Protein concentrations injected varied from 2–6 mg/ml. The pipette-microinjection technique of Graessmann and Graessmann (9) as modified by Zavortink et al. (46) was used to deliver ~1/10 cell volumes. We have previously determined the average injection volume by microinjecting large numbers of cells with ^{125}I-BSA and counting in a liquid scintillation counter (46). Assuming that the endogenous tubulin concentration is ~2 mg/ml (10), we calculate that the molar in vivo ratio of injected tubulin to endogenous tubulin ranged from 1:10 to 1:3. Cells grown on coverslips were observed during microinjection with a × 40, phase contrast, water immersion lens (numerical aperture 0.75) on a Zeiss Universal microscope. For FRAP studies, cells were injected at room temperature (22°C) then transferred to a 37°C CO_2 incubator for between 30 min and 24 h to allow incorporation and equilibration. They were then mounted in tissue culture medium on slides using strips of parafilm for spacers and a mixture of parafin, petroleum jelly, and lanolin (1:1:1) as a sealant. Microinjected cells mounted in this manner survived for up to 3 d.

For DTAF-tubulin incorporation studies, metaphase and prophase cells grown on glass coverslips were injected and observed at 37°C in an open, controlled environment chamber. HEPES buffered (20 mM) culture medium perfusion through the chamber was effected by a syringe pump and tygon tubing jacketed with flowing, heated water. A microthermistor probe (Yellow Springs Instrument Co., Yellow Springs, OH) suspended in the medium just above the cells was used to monitor chamber temperature and to regulate the temperature of the water jacket. With a culture medium flow rate of 2 ml/min, pH change was negligible and cells remained in good health in the open chamber for many hours. For interphase DTAF-tubulin incorporation studies, cells grown on glass coverslips were injected in the controlled environment chamber, then mounted on slides, and sealed for observation with a high resolution oil immersion lens (see below). During observation a model 279 Sage air curtain incubator (White Plains, NY) was used to maintained the cells at 36 ± 1°C.

Fluorescence Redistribution After Photobleaching (FRAP): Photobleaching was performed and fluorescence redistribution observed with a × 63 planapochromat lens (numerical aperture 1.4) on a Zeiss Universal microscope as described by Salmon et al. (32). Briefly, microinjected cells were aligned to receive a small circular column of light from the 488-nm line of an argon laser on selected regions of their fluorescent mirotubule arrays. The redistribution of fluorescence into the resulting photobleached spot was recorded by taking 0.5-s 35-mm photographs of a television monitor displaying the signal produced by a Venus DV II intensified television camera. The diameter of the photobleaching beam was controlled by placing a 100-μm electron microscope aperture in the laser beam path at the aerial image plane in the epi-illuminator. The columnar nature of the resulting beam (approximate diameter = 3 μm) at the specimen plane is seen in Fig. 1.

Data Analysis: The 35-mm negatives which recorded the changes in fluorescence intensity distributions during incorporation and FRAP studies were analyzed with a Joyce-Loebl scanning microdensitometer model 3C. The resulting distributions of optical density versus position were processed as described by Salmon et al. (30) in an accompanying paper. The half times ($t_{1/2}$s) of fluorescence incorporation and FRAP were determined by fitting a single exponential curve of the form $I/I_{max} = 1 - e^{-kt}$ to the data, using a non-linear, least-squares method. The term I represents fluorescence intensity at time t, I_{max} represents the fluorescence intensity at t = infinity, and k is the time constant for the curve.

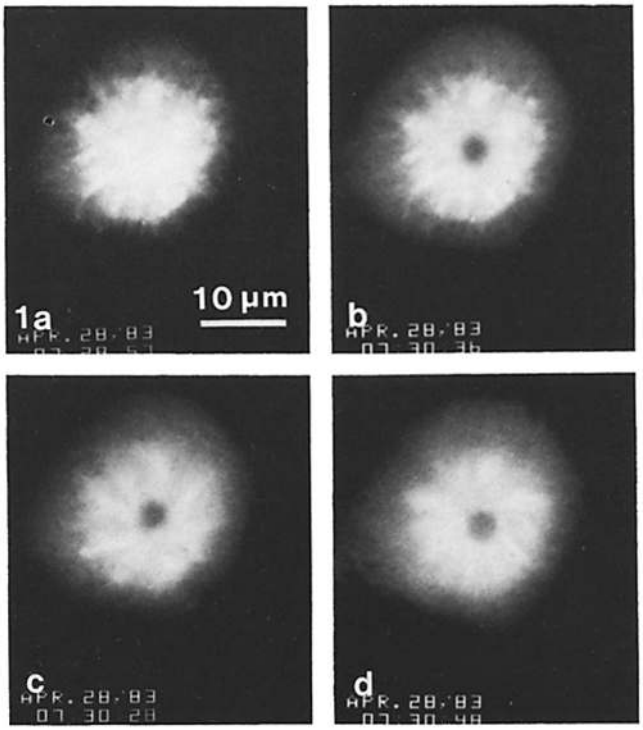

FIGURE 1 The columnar nature of the photobleaching beam. (*a*) The spindle of a fixed BSC mitotic cell incubated with monoclonal antitubulin antibody and stained with fluorescent goat antimouse antibody (spindle viewed end-on). (*b*) At the same focal plane after photobleaching. (*c*) 4 μm above the original plane of focus. (*d*) 4 μm below the original plane of focus. × 1,100.

Indirect Immunofluorescence: Microinjected cells on coverslips were prepared for indirect immunofluorescence staining by rinsing briefly in phosphate buffered saline (PBS) (37°C), lysing for 30 s in 0.1 M PIPES, 1 mM $MgCl_2$, 1 mM EGTA, 0.5% Triton × 100, at pH 6.9 and 37°C, and fixing for 5 min in −20°C anhydrous methanol. Fixed cells were rehydrated in PBS, incubated for 10 min at room temperature with a 1:50 dilution of monoclonal antitubulin antibody (a generous gift of Dr. J. V. Kilmartin, MRC Laboratory of Molecular Biology, Cambridge, England, reference 16), washed 6 × in PBS (10 s each), and incubated for 10 min at room temperature with a 1:500 dilution of rhodamine-labeled goat anti-mouse antibody (Miles Laboratories, Elkhart, IN). Coverslips were washed 6 × in PBS, mounted with 90% glycerol, 0.1 M $NaHCO_3$, 2% *N*-propyl gallate, at pH 8.2 (8), and sealed with clear nail polish. The staining method was designed to produce a faint, tubulin-specific rhodamine signal, thus minimizing "bleed-through" into the flourescein channel during photomicrography. Cells were observed and recorded using a 63× planapo lens, with a Zeiss Photomicroscope III. Photomicrographs were taken with Kodak Tri-X film and developed in Diafine.

High Voltage Electron Microscopy: Cells grown on Formvar-coated gold finder grids were prepared for whole mount, high voltage electron microscopy by extraction for 2 min at 37°C in the lysis buffer described above and fixation for 15 min in Hank's balanced salt solution (HBSS) at pH 7.0 with 0.1 mM GTP and 2.8% glutaraldehyde. Cells were rinsed in HBSS and transferred to 1% OsO_4 for 2 min, rinsed and transferred to 0.2% tannic acid for 15 min, rinsed and transferred to 2% uranyl acetate for 3 min, then rinsed and dehydrated in ethanol. Finally cells were critical-point dried (1), carbon coated, and examined with the JEM-1000 high voltage electron microscope at the national facility in Boulder, Colorado.

RESULTS

Indirect Immunofluorescence of Microtubules in Microinjected Cells

The fibrous patterns of fluorescein fluorescence observed after microinjection of DTAF-tubulin into cultured mam-

malian cells were compared with the patterns of rhodamine fluorescence produced in the same cells with antitubulin antibody. Microinjected cells were lysed, then fixed and stained with antibodies as described in Materials and Methods. Images of microinjected cells generated first with fluorescein and second with rhodamine excitation illumination are shown in Fig. 2. The contribution of the rhodamine signal to the fluorescein signal was minimal. Individual fibers are difficult to distinguish in the fluorescein images (direct visualization of fixed DTAF-tubulin) but the patterns are strikingly similar to the rhodamine images (visualization of all fixed tubulin by immunofluorescence) at all stages of the cell-cycle. An interesting difference in the two images of tubulin localization is seen in the midbody (Fig. 2, *g* and *h*). DTAF-tubulin is distributed throughout the intercellular bridge but antibody to tubulin does not stain well in the equatorial zone. This lack of microtubule staining has been previously reported (4) and is thought to be due to the fact that the interdigitating microtubules seen there by electron microscopy are surrounded by dense osmiophilic material which excludes antibody (23, 26). A more subtle reduction of antitubulin staining relative to DTAF-tubulin fluorescence is seen in the midzone of the anaphase spindle (Fig. 2, *e* and *f*), in the prometaphase asters (Fig. 2, *c* and *d*), and around the interphase microtubule organizing center (Fig. 2, *a* and *b*). It may be that antibody is excluded from these regions as it is at the equatorial zone of the intercellular bridge. Note however, that some of the differences in the two images of tubulin distribution in the prometaphase and interphase cells are due to slight differences in their planes of focus.

We have tested whether the fibrous fluorescence patterns that develop in living cells following microinjection of DTAF-tubulin are due specifically to the polymerization of tubulin by observing fluorescence patterns in three control experiments: (*a*) the microinjection of fluorescent proteins other than tubulin; (*b*) the microinjection of polymerization incompetent, fluorescent microtubule proteins (MTP) (which include high molecular weight aggregates, polymerization incompetent microtubule-associated proteins and tubulin, and free DTAF); and (*c*) the comparison of the drug sensitivities of DTAF-tubulin patterns with those of microtubules. RITC-labeled actin microinjected into mitotic BSC cells produced general, diffuse fluorescence patterns (Fig. 3) that were not similar to fibrous DTAF-tubulin patterns. Similar diffuse fluorescence patterns were seen in mitotic and interphase cells microinjected with rhodamine- or fluorescein-labeled ovalbumin, BSA, and rabbit immunoglobulin (data not shown). No evidence of autophagy of these injected proteins was seen within the time frame of observation (0.5–2 h). Microinjection of polymerization incompetent DTAF-MTP, as reported by others (15, 38), produced punctate cytoplasmic fluorescein patterns, perhaps due to autophagy (33), and bright nuclear staining probably due to the binding of free DTAF by nuclear components. The polymerization incompetent DTAF-MTP did not incorporate to any observable extent into microtubules seen in the same cell by rhodamine immunofluorescence (Fig. 4). Finally, when interphase cells displaying fibrous DTAF-tubulin patterns were perfused with 7 μM Nocodazole, there was a transition to a diffuse, nonfibrous pattern over the course of an hour. When mitotic cells were treated in the same manner, spindle fluorescence faded and cytoplasmic background fluorescence increased over the course of a few minutes implying a shift of DTAF-tubulin from polymer to free dimer forms. During this transition spindle poles in metaphase cells collapsed inward toward the metaphase plate (Fig. 5, *a–c*). When cells microinjected with DTAF-tubulin were perfused with 10 μM Taxol, fluorescence patterns consistent with the effects of Taxol on mammalian cells, as described by DeBrabander (7), were produced. Microtubules in Taxol-treated interphase cells appeared bundled while mitosis was characterized by multiple aster-like structures (Fig. 5, *e* and *f*). Evidence of interphase bundling began to appear after an hour of perfusion while changes in spindle morphology occurred more quickly. Dislocation of half spindles from their normal metaphase positions was seen within 2 min.

The Ability of DTAF-Tubulin to Function in Vivo

Cells microinjected with DTAF-tubulin were observed through an entire cell cycle. The DTAF-tubulin participated in the formation of all microtubule-related structures at all stages of interphase and mitosis with no apparent effect on viability. BSC cells incorporated DTAF-tubulin into fluorescent interphase microtubule arrays over the course of an hour. At 24 and 48 h daughter cells showed distinct fibrous interphase arrays of reduced fluorescence intensity. PtK_1 cells injected at prophase exhibited fluorescent asters within a minute. Characteristic fluorescent spindle arrays formed as cells proceeded through mitosis, forming daughters connected by a fluorescent midbody. During the subsequent interphase the cells contained a fluorescent cytoplasmic microtubule complex, and daughter cells observed in mitosis at 24 h exhibited fluorescent mitotic arrays of reduced intensity (data not shown).

Incorporation Rates of DTAF-Tubulin

The rate of incorporation of DTAF-tubulin into microtubules was found to depend on the cell-cycle stage of the microinjected cell. Using the controlled environment chamber described in Materials and Methods, we injected metaphase, prophase, and interphase cells and monitored the rates at which their microtubules became fluorescent (Fig. 6). The images, taken at various times following microinjection of prophase or metaphase cells, were analyzed as described by Salmon et al. (30). The $t_{1/2}s$ of fluorescence incorporation, hence of DTAF-tubulin incorporation (30), were calculated from the parameters of the best fitting exponential curves. We have not yet developed a system that can quantitate the incorporation of DTAF-tubulin by interphase microtubules because they are not concentrated in discrete structures as mitotic microtubules are. Time intervals that are likely to bracket the interphase incorporation $t_{1/2}s$ were estimated by studying image series as seen in Fig. 6, *a–c*. The elapsed time between an injection and the first image showing a faint fibrous fluorescence in the cell rather than a general diffuse fluorescence was taken to represent the early boundary of a $t_{1/2}$ interval (Fig. 6 *a*). The elapsed time between injection and the first image in which the cell's fibrous pattern was apparently fully developed was taken to represent the late boundary of a $t_{1/2}$ interval (Fig. 6 *c*).

With our current methods of analysis we can discern no significant difference in the rates of DTAF-tubulin incorporation at metaphase and prophase. The $t_{1/2}s$ for six metaphase cells (PtK_1) vary from 6 to 38 s (mean = 18 ± 14 s). Values for 10 prophase cells (PtK_1) range from 4 to 22 s (mean = 14 ± 7 s). As described in Materials and Methods, there is a time

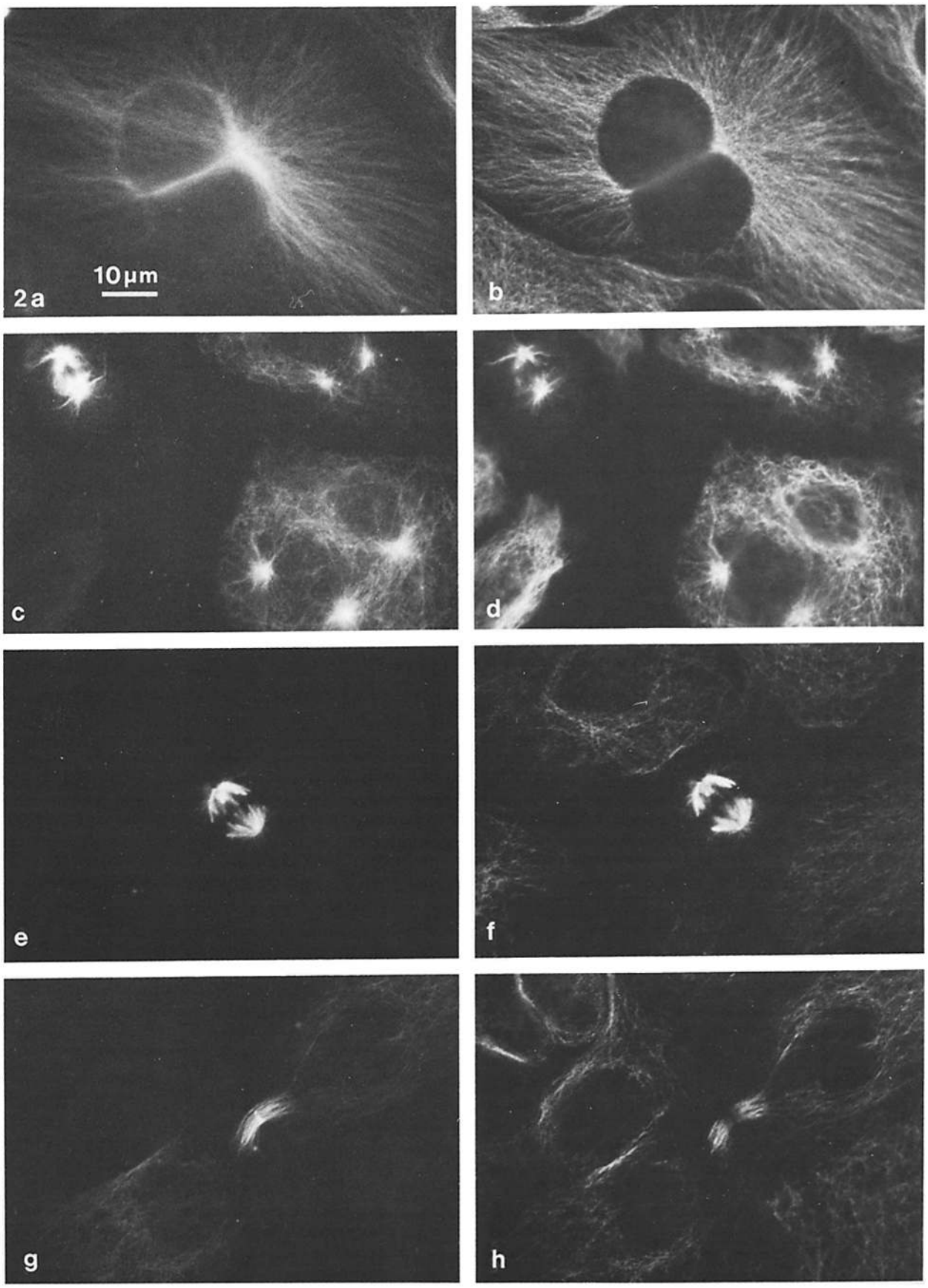

FIGURE 2 Comparison of fibrous DTAF-tubulin patterns with microtubule patterns in microinjected cells. Cells microinjected with DTAF-tubulin were lysed and fixed after equilibration times of 30 min for mitotic cells and 3 h for interphase cells. Fixed

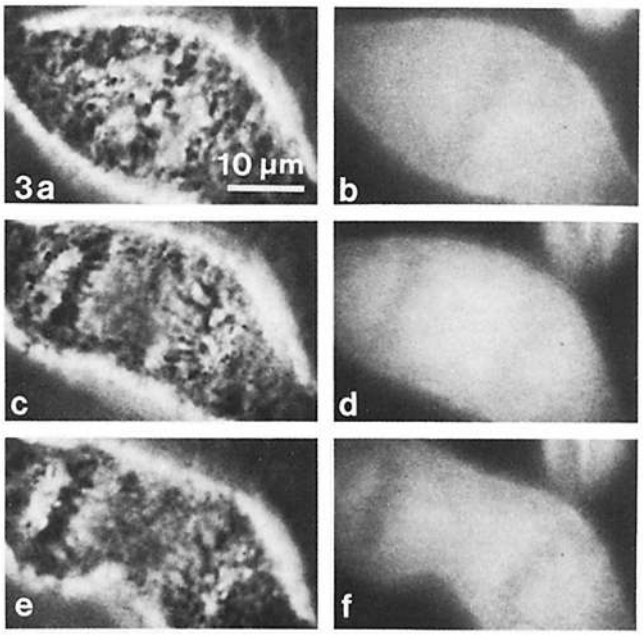

FIGURE 3 Fluorescence patterns of a mitotic BSC cell microinjected with rhodamine-labeled actin observed at different stages of mitosis. On the left are phase contrast images and on the right are fluorescence images. (*a* and *b*) metaphase; (c and *d*) anaphase; (e and *f*) telophase. × 1,100.

lag between the microinjection of an interphase cell using the × 40 water immersion lens and the first observation with the × 63 oil immersion lens. Use of the × 63 lens is necessary to obtain high space-resolution of the interphase microtubule arrays. In 5 of the 11 BSC cells followed it was evident that the $t_{1/2}$ of incorporation had been passed before the first observation with the high resolution lens (14–22 min). In these cases the early boundary of a $t_{1/2}$ interval was taken as zero and the late boundary as the time of the first image. In the remaining six cells the $t_{1/2}$ intervals range between 15 and 52 min. A rough value of the $t_{1/2}$ of incorporation of DTAF-tubulin into interphase MTs of 20 ± 12 min is taken from the mean of the $t_{1/2}$ interval midpoints.

Fluorescence Redistribution After Photobleaching of DTAF Tubulin

FRAP was selected as a second method of studying tubulin dynamics because it complements the incorporation rate experiments in two ways. First, FRAP experiments are performed on cells that have been allowed to equilibrate after microinjection. Second, in contrast to results from interphase incorporation, interphase FRAP can be analyzed in the same quantitative manner as FRAP in mitotic cells. The results of FRAP studies are analogous to those of the incorporation rate studies in that the rate of FRAP of DTAF-tubulin was found to be dependent on cell-cycle stage.

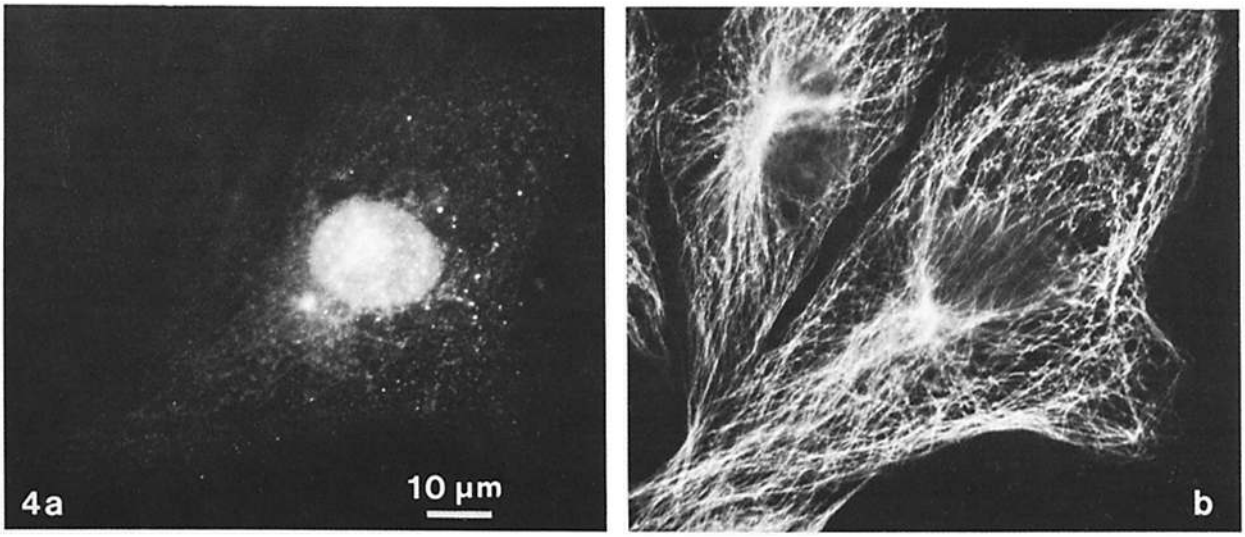

FIGURE 4 Comparison of the distribution of microinjected polymerization incompetent DTAF-MTP with the distribution of microtubules. BSC interphase cells were microinjected, allowed to equilibrate for 2 h, then lysed, and fixed. Fixed cells were incubated with monoclonal antitubulin antibody and stained with rhodamine-labeled goat anti-mouse antibody. (*a*) An interphase cell viewed with fluorescein excitation illumination (visualization of DTAF-labeled high molecular weight aggregates, polymerization incompetent MAPs and tubulin, and free DTAF). The nuclear staining is probably due to the binding of free DTAF by nuclear components. (*b*) The same cell viewed with rhodamine excitation illumination (visualization of microtubules). × 870.

cells were incubated first with monoclonal antitubulin antibody and then stained with rhodamine-labeled goat anti-mouse antibody. Images on the left were produced with fluorescein excitation illumination (visualization of DTAF-tubulin). Images on the right were produced with rhodamine excitation illumination of the same field (visualization of all fixed tubulin). Bleed-through was minimal as can be seen by examining the very faint fluorescein images of cells that were not microinjected with DTAF-tubulin. (*a* and *b*) A binucleate BSC interphase cell. In the upper right a portion of another microinjected interphase cell can be seen. (c and *d*) Two PTK_1 mitotic cells at prophase and one at prometaphase. (e and *f*) A PTK_1 early anaphase cell. (*g* and *h*) PTK_1 daughter cells joined by a midbody. × 1,000.

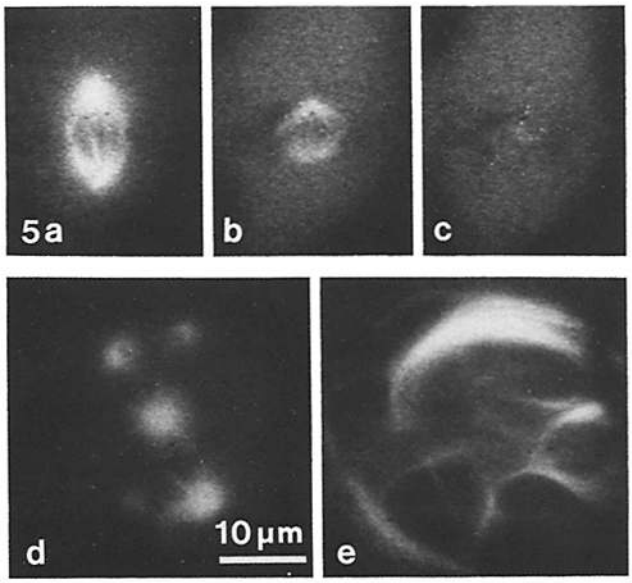

FIGURE 5 The responses of DTAF-tubulin fluorescence patterns to nocodazole and taxol perfusion. Cells were microinjected with DTAF-tubulin and allowed to equilibrate before drug treatments. (*a*) A PTK_1 metaphase cell before perfusion; (*b*) the same cell 55 s after; and (*c*) 180 s after perfusion with 7 μM nocodazole; (*d*) A PTK_1 mitotic cell 12 h after; and (*e*) a PTK_1 interphase cell 12 h after perfusion with 10 μM taxol. *a*, *b*, and *c* were photographed and printed under identical conditions. × 1,100.

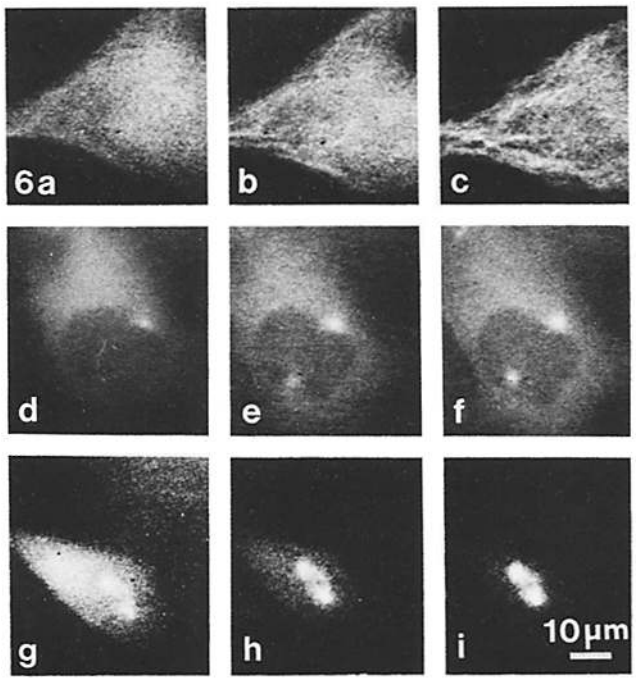

FIGURE 6 The incorporation of microinjected DTAF tubulin. Cells were microinjected with DTAF-tubulin and the changes from diffuse fluorescence patterns to organized microtubule-like fluorescence patterns were followed with a video imaging system. The images are of: A BSC interphase cell (*a*) at 21 min; (*b*) at 28 min; and (*c*) at 41 min after microinjection. A PTK_1 prophase cell at (*d*) 10 s; (*e*) 58 s; and (*f*) 240 s after microinjection. A PTK_1 metaphase cell at (*g*) 6 s; (*h*) 20 s; and (*i*) 48 s after microinjection. The three images of the prophase cell and of the metaphase cell were photographed and printed under identical conditions. × 550.

In FRAP studies mitotic cells were usually incubated at 37°C for 30 min after microinjection to allow equilibration. Interphase cells were usually incubated for 2–8 h. In neither case were results noticeably effected by increasing incubation times to 24 h. The 488-nm line of a 2-W argon laser was used at full power to irreversibly photobleach the fluorescence from selected regions of microtubule arrays in interphase, prophase, and metaphase cells (Fig. 7). The laser pulse duration was varied from 0.5 s to 0.05 s in different experiments. The length of the pulse did not seem to effect the results, but the 0.05-s pulse was used in most experiments.

It is evident from the images of Fig. 7 that the fluorescence intensity of an entire cell is reduced by the photobleaching event. Part of this reduction is due to a slight diffraction of the column of laser light caused by its passage through the 100-μm aperture described in Materials and Methods. This diffracted light strikes the specimen outside the 2 μm targeted spot. Some of the reduction is also due to the fact that the fraction of the total DTAF-tubulin in a cell that is within the targeted spot is irreversibly photobleached. The percentage lost is especially large in a metaphase half spindle bleach because most of the cell's fluorescent tubulin is concentrated within the spindle. Other factors contributing to the generalized photobleaching are the scattering of laser light within the cell by cell structures and the 0.7-s periods of epiillumination necessary to record images during redistribution (30).

Redistribution of fluorescence into bleached spots after laser irradiation was recorded and analyzed by the same methods used for the studies of rates of DTAF-tubulin incorporation by mitotic cells. The change in relative fluorescence intensity of the photobleached spot was determined as a function of time; data points were used to define a single exponential recovery curve for each cell (30). As in the incorporation rate studies, the $t_{1/2}s$ for interphase microtubules are markedly longer than those of mitotic microtubules (Fig. 8). FRAP $t_{1/2}$ values for 10 metaphase cells (PTK_1) varied from 3 to 22 s (mean = 11 ± 6 s), for 10 prophase cells (PTK_1) from 1.4 to 31 s (mean = 14 ± 10 s), and for 17 interphase cells (BSC) from 92 to 320 s (mean = 200 ± 85 s).

To see if the differences in rates of FRAP for mitotic versus interphase cells were a result of the different cell types used, FRAP studies were also performed on BSC metaphase and PTK_1 interphase cells. Due to the thickened morphology of these cells the contrast in fluorescence intensity between microtubules and cytoplasm is poor but FRAP results can be analyzed. BSC metaphase FRAP $t_{1/2}s$ (mean = 13 ± 7 s, n = 6) fall in the same range as PTK_1 metaphase values and PTK_1 interphase FRAP $t_{1/2}s$ (mean = 270 ± 73 s, n = 4) fall in the same range as BSC interphase values. This shows that the differences between PTK_1 mitotic FRAP $t_{1/2}s$ and BSC interphase FRAP $t_{1/2}s$ are due to differences between mitosis and interphase not due to the different cell types used.

It is evident in mitotic FRAP experiments that the major portion of fluorescence and of fluorescence redistribution is associated with microtubules in an aster or the spindle. The contrast between background cytoplasmic fluorescence (DTAF-tubulin in free dimer form) and a spindle or an aster is high (Fig. 7, *e–l*). Interphase microtubules are usually distributed throughout a cell's cytoplasm rather than concentrated in the discrete structures seen in mitotic cells. Therefore, the contrast between microtubule fluorescence and background cytoplasmic fluorescence is not high. The fibrous

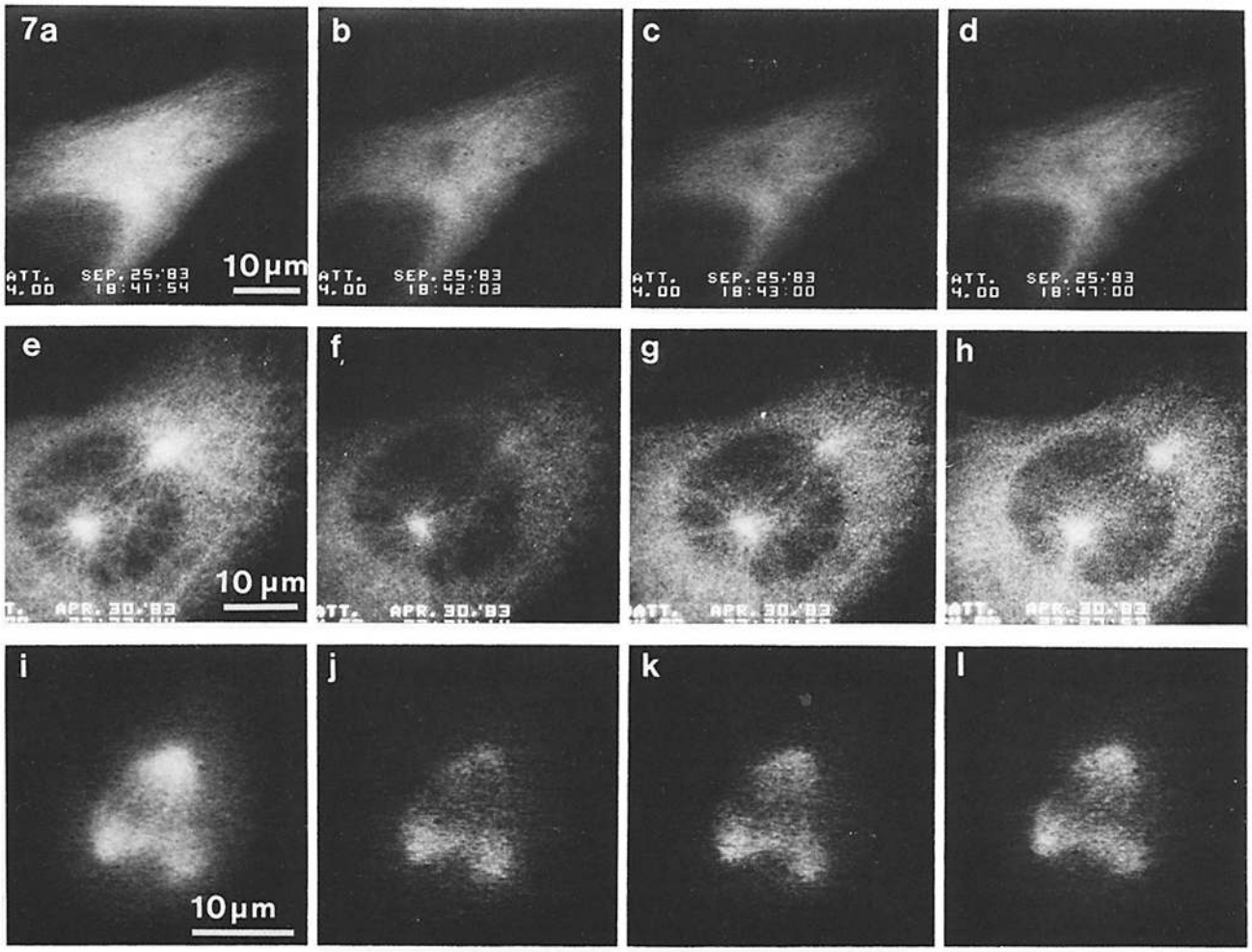

FIGURE 7 Fluorescence redistribution after photobleaching (FRAP) of cells microinjected with DTAF-tubulin. Cells were incubated for 0.5–24 h after microinjection to allow incorporation of the DTAF-tubulin and then photobleached with a 2-μm diam column of 488 nm light from an argon laser. Redistribution of fluorescence into the photobleached spot was followed with a video imaging system. The images are of a BSC interphase cell (a) 6 s before; (*b*) 3 s after; (*c*) 60 s after; and (*d*) 300 s after photobleaching. The interphase cell does not show complete fluorescence redistribution into the photobleached spot (*d*). All interphase cells observed for extended periods after photobleaching did show complete redistribution. × 920. A PTK_1 prophase cell (e) 27 s before; (*f*) 3 s after; (*g*) 48 s after; and (*h*) 220 s after photobleaching. × 1,000. A PTK_1 metaphase cell (*i*) 5 s before; (*j*) 3 s after; (*k*) 27 s after; and (*l*) 92 s after photobleaching. × 1,400. A tripolar metaphase cell was selected to show that spindle rotation is not a factor in fluorescence redistribution.

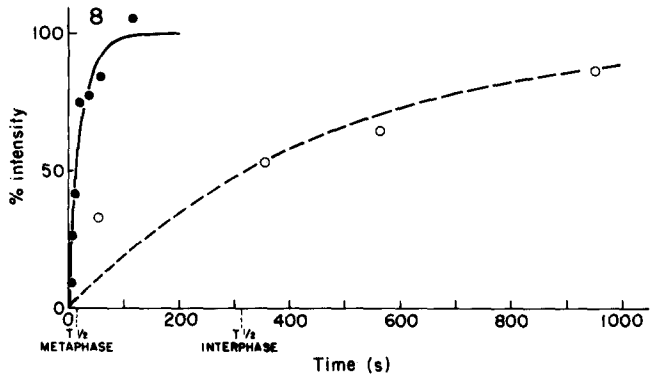

FIGURE 8 Comparison of FRAP rates for a metaphase and an interphase cell. Examples of relative fluorescence intensity plotted against time after photobleaching for a metaphase cell (●) and an interphase cell (○). Circles represent data points determined by microdensitometry of negatives. Lines represent best fitting curves using the function $I/I_{max} = 1 - e^{-kt}$ (30). The $t_{1/2}$ for each curve is noted on the X axis.

quality of the fluorescence seen by direct observation in an interphase cell is mostly lost in video images obtained at the low excitation illumination levels which permit the recording of multiple images from the same cell. To determine whether or not interphase FRAP represents a microtubule related phenomenon, we have carried out two different types of control experiments. Interphase cells were microinjected with fluorescein labeled ovalbumin (45 kd) or fluorescein labeled rabbit immunoglobulin (150 kd). The cells were allowed to equilibrate for 2–6 h and used for FRAP experiments. The redistribution of fluorescence into spots photobleached in the cells occurred so rapidly that we were unable to record enough images to determine accurately the increase in fluorescence intensity as a function of time. In no case, however, did a distinguishable spot remain after a few seconds. This implies that the slow redistribution of fluorescence in interphase cells microinjected with DTAF-tubulin (110 kd) is due to properties unique to the DTAF-tubulin. A second series of control FRAP experiments were performed on cells microinjected with DTAF-tubulin and perfused with 7 μM Nocodazol. The

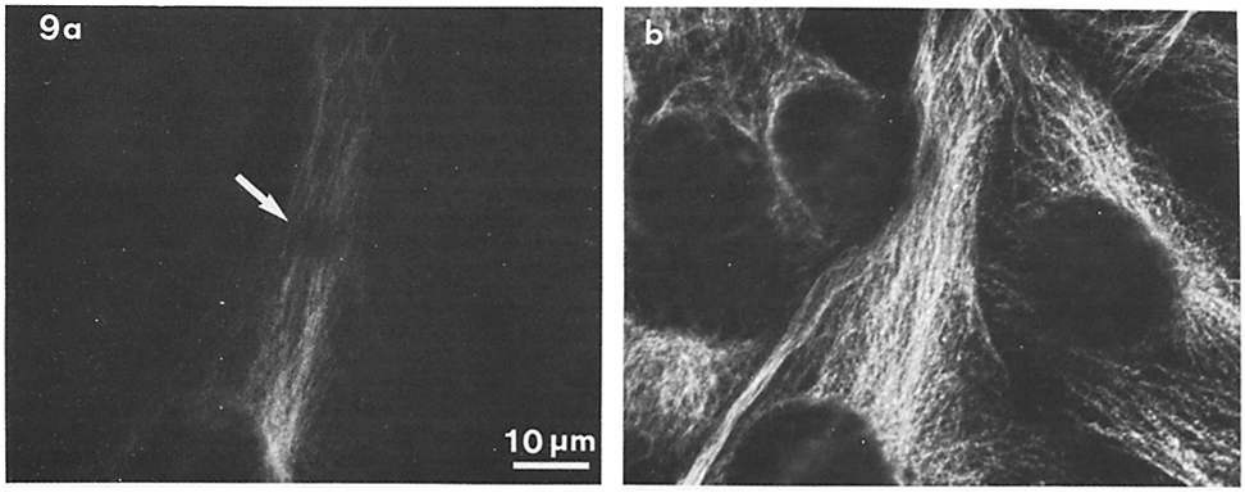

FIGURE 9 The distribution of microtubules within a photobleached spot. Cells were microinjected with DTAF-tubulin, incubated for 3 h, photobleached, immediately lysed, fixed, incubated with monoclonal antitubulin antibody, and stained with rhodamine-conjugated secondary antibody. (*a*) The location of the photobleached spot (arrow) is seen by fluorescein excitation illumination (visualization of DTAF-tubulin). (*b*) The distribution of microtubules is seen by rhodamine excitation illumination. There is no apparent disruption of microtubules within or near the photobleached spot. × 1,000.

redistribution of fluorescence into photobleached spots was again too rapid to analyze with our current system. This implies that the slow redistribution of fluorescence in interphase cells is due to the properties of DTAF-tubulin that are sensitive to Nocodazol. It is probable, therefore, that the slow redistribution recorded in interphase DTAF-tubulin FRAP is due to the presence of microtubules.

The Effects of Photobleaching in Vivo

We have studied the effects of DTAF-tubulin photobleaching on two readily observed functions of cultured cells; mitotic division and particle saltation. Mitotic cells followed after spindle FRAP invariably complete mitosis and cytokinesis. Occasionally metaphase cells begin anaphase chromosome separation and spindle elongation during the period of fluorescence redistribution. Particle saltation in interphase cells microinjected with DTAF-tubulin was followed after photobleaching. Laser pulses of 0.5, 5.0, and 45 s have no visible effect on particle saltation within or near the photobleached spots.

To determine whether photobleaching in vivo destroys or damages microtubules containing DTAF-tubulin, we have used double label fluorescence microscopy and electron microscopy. With the light microscope we have compared microtubule patterns seen by indirect immunofluorescence with DTAF-tubulin patterns in photobleached cells. BSC interphase cells were injected with DTAF-tubulin, allowed to equilibrate, and photobleached as in FRAP studies. Immediately after photobleaching (within 5 s), cells were lysed and fixed. After incubation with antitubulin antibody and rhodamine-labeled secondary antibody, individual cells were observed with the appropriate optics to distinguish the two fluorochromes. Examples of fluorescein and rhodamine images of a photobleached cell are seen in Fig. 9. A distinct dark spot produced by laser irradiation can be seen in the DTAF-tubulin image but examination of the rhodamine antitubulin pattern shows no distinguishable changes in the normal distribution of microtubules within or near the photobleached spot.

To obtain higher resolution images of photobleached microtubules than are afforded by the light microscope, a high voltage electron microscope was used in experiments similar to the one just described. BSC interphase cells grown on Formvar coated, gold finder grids were injected with DTAF-tubulin, allowed to equilibrate, and photobleached as in FRAP studies. Improvements in our perfusion technique allowed us to initiate lysis within 2 s after photobleaching. During lysis, phase and fluorescence video images were taken to record the location of photobleached spots. After fixation, staining, and critical point drying (see Materials and Methods), cells were examined with a high voltage electron microscope. In the six cells examined it has not been possible to locate a photobleached area by searching an electron micrograph for regions of morphological heterogeneity. It was necessary to map the location of bleached spots onto electron micrographs from the video images. Fig. 10 is an enlargement of a portion of such a photobleached area. Microtubules are abundant and appear undamaged.

It is possible that photobleaching of DTAF-tubulin in vivo damages microtubules or otherwise alters tubulin dynamics in ways not discernible in our fluorescence and electron micrographs. If this is so, one would expect the change in dynamics to be proportional to the number of fluorophores bleached (43). Variation of the laser pulse between 0.05 and 0.5 s does not appear to alter metaphase or interphase FRAP $t_{1/2}$s. In addition, when up to three FRAP series are recorded from the same spot in a cell, allowing for full redistribution between, there is no consistent shift of $t_{1/2}$s. We have also determined metaphase incorporation $t_{1/2}$s of DTAF-tubulin that has been bleached in vitro to 80% of its original fluorescence intensity (19). The values obtained (mean = 24 ± 10 s, n = 4) fall within the range of those resulting from the injection of unbleached DTAF-tubulin.

DISCUSSION

We have shown using two different approaches that the apparent rate of exchange in vivo of free DTAF-tubulin with DTAF-tubulin in polymer is markedly faster in mitotic cells

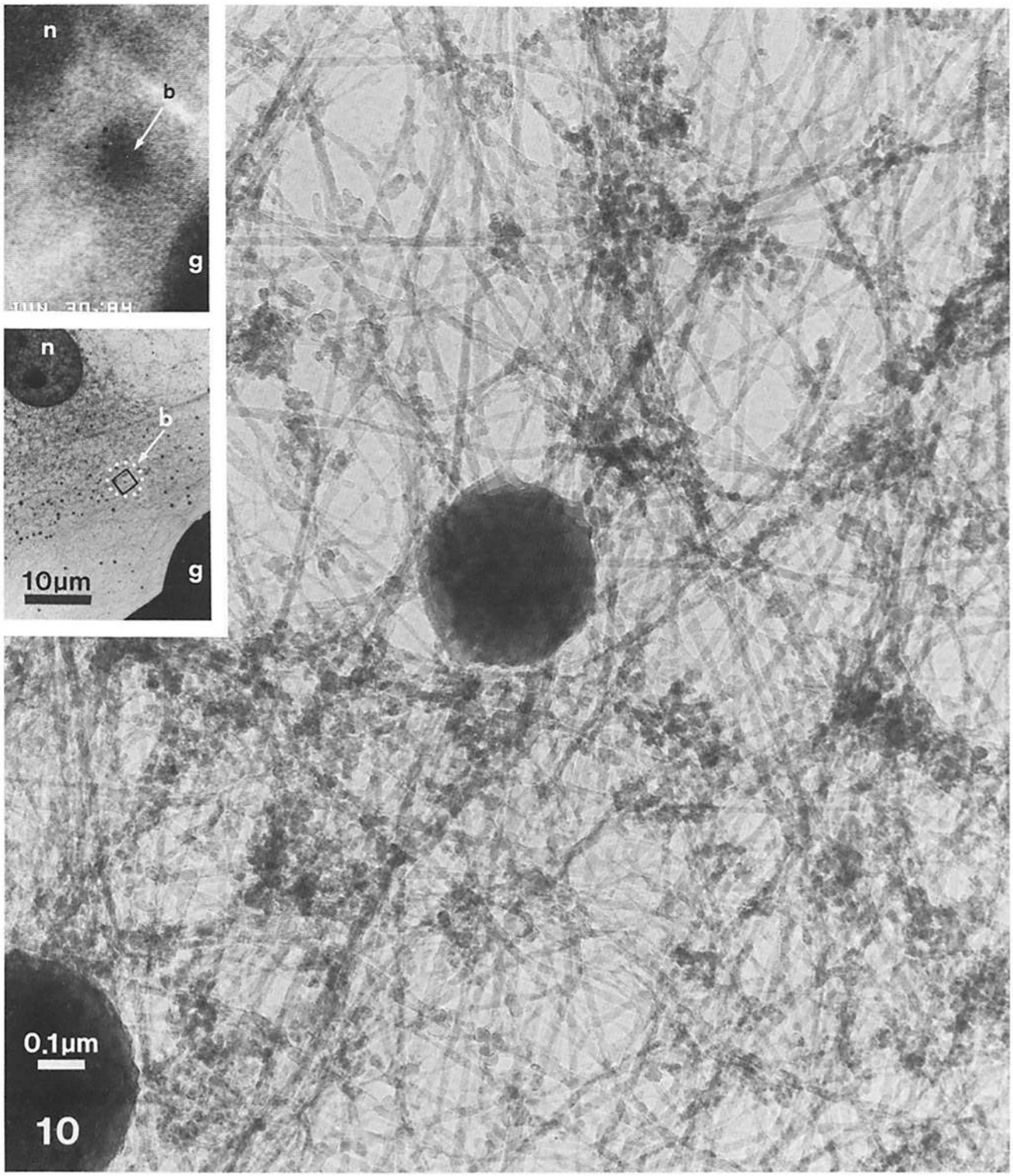

FIGURE 10 High voltage electron micrograph of microtubules in the photobleached region of a BSC cell. Cells were injected with DTAF-tubulin and incubated for 3 h. An interphase cell was photobleached, lysed within 2 s of photobleaching, and prepared for electron microscopy. Fluorescence (*upper inset*) and phase contrast (not shown) images were recorded during lysis. It was possible to define the area of photobleached fluorescence in electron micrographs (circle of white dots, *lower inset*) by its position in video micrographs relative to prominent features like the cell nucleus (*n*) and the grid bar (*g*). The diameter of the large filaments is consistent with their identification as microtubules. We did not observe fragmentation or other major damage to microtubules in the photobleached area or any difference in morphology relative to the remainder of the cell. The small black square in the lower inset encloses the area seen at high magnification. × 80,000; (*insets*) × 1,200.

than in interphase cells. The mean half-time for incorporation of microinjected DTAF-tubulin by microtubules in metaphase cells is ~70-fold shorter than that estimated for microtubules in interphase cells. Prophase asters incorporate fluorescence at rates indistinguishable from metaphase spindles. Fluorescence redistribution after photobleaching (FRAP)

studies with cells that have been allowed to equilibrate for up to 24 h after injection indicate similar relationships between the apparent rates of exchange at the three different cell-cycle stages. The mean half-time of FRAP of metaphase microtubules is 18 times shorter than that of interphase microtubules. FRAP $t_{1/2}s$ of prophase asters are not distinguishable from those of metaphase spindles.

One's confidence in rates of incorporation and FRAP as manifestations of normal in vivo tubulin dynamics depends on the controls for the DTAF-tubulin probe and for the specific methods of study. We have shown through fluorescein-rhodamine double labeling that the patterns of fluorescence produced by microinjected DTAF-tubulin are nearly indistinguishable from the microtubule patterns seen with antitubulin immunofluorescence. Furthermore, it is clear that the formation of fibrous DTAF-tubulin patterns is dependent on characteristics specific to tubulin. Microinjected fluorescent actin, BSA, ovalbumin, immunoglobulin, and polymerization incompetent DTAF-microtubule proteins do not produce microtubule-like patterns. Also, the responses of DTAF-tubulin patterns to Nocodazole and Taxol are consistent with the responses of normal microtubule patterns observed by immunofluorescence (6, 7). Coupled with the in vitro results of Leslie et al. (19), which indicate that DTAF-tubulin does not bind adventitiously to the walls of pre-existing microtubules, our findings clearly support the published conclusion (15, 38) that DTAF-labeled bovine neurotubulin can participate in the formation of microtubules in vivo. In addition we have observed that DTAF-tubulin takes part in the formation of microtubules throughout the cell cycle and can persist in this activity for at least 48 h following microinjection. Although minor differences in the behavior of labeled and unlabeled protein may certainly exist, by currently available criteria DTAF-tubulin is functionally indistinguishable from endogenous tubulin in vivo. We therefore believe that DTAF-tubulin is a valid probe for studying normal in vivo tubulin dynamics.

Studying tubulin dynamics by observing incorporation rates involves the microinjection of DTAF-tubulin and its immediate observation. The injection of 1/10 of a cell volume of DTAF-tubulin dimer at concentrations ranging up to 6 mg/ml represents an approximate 30% increase in cellular tubulin. This probably constitutes a perturbation of a cell's normal dimer-polymer tubulin equilibrium. The observed rates of incorporation may thus represent the formation of new polymer as well as the exchange of free DTAF-tubulin with unlabeled tubulin in existing polymer. If an equilibrium perturbance does result from microinjection however, its effects are not observable as an interruption in the normal progress of mitosis and cytokinesis.

The FRAP investigation was designed to examine rates of exchange of free tubulin dimers with tubulin dimers in polymer in cells that were not perturbed by the effects of recent microinjection. We have studied the possibility that the act of photobleaching or the presence of photobleached DTAF-tubulin might perturb microinjected cells' normal functions or damage their microtubules. We have observed that anaphase chromosome movement in mitotic cells and particle saltation in interphase cells are not noticeably affected by laser irradiation. In an accompanying paper we have shown that photobleaching of fluorescent microtubules in vitro does not result in appreciable depolymerization or fragmentation. Under photobleaching conditions chosen to simulate those in a microinjected cell there is no major change in tubulin's polymerization-depolymerization behavior (19). In another accompanying paper we have shown that photobleaching of a mitotic cell does not result in an observable shift in spindle birefringence (30). In this paper we have examined microtubules within photobleached spots in BSC interphase cells by immunofluorescence and high voltage electron microscopy. No change in microtubule distribution as a result of photobleaching is seen in immunofluorescence or low magnification electron micrographs. High magnification electron micrographs of photobleached areas show no evidence of microtubule fragmentation or distortion. Although these results do not eliminate the possibility of damage below the limit of resolution, they support our view that FRAP represents the normal exchange of free tubulin with tubulin in polymer, not the photobleach-induced destruction and repair of polymer. Also, if photobleaching damages DTAF-tubulin in a way that affects its dynamic behavior one would expect to see a change in the observed dynamics that is proportional to the number of fluorophores bleached (43). Neither does shifting the duration of laser irradiation from 0.05 to 0.5 s nor does photobleaching the same area in a cell more than once result in a significant shift in FRAP $t_{1/2}s$. We have also shown that the presence within a cell of increased amounts of photobleached DTAF-tubulin does not result in a significant shift in incorporation rates. Our examination of the DTAF-tubulin probe and of the effects of the methods of incorporation and FRAP studies support the notion that FRAP and incorporation rates represent normal in vivo tubulin dynamics.

Additional support is found in the similarity of results obtained using the two different methods. The mean $t_{1/2}s$ of incorporation and FRAP in mitotic cells are virtually the same and the mean $t_{1/2}s$ of incorporation and FRAP in interphase cells are both significantly longer than the mitotic values although by incorporation the difference is 70-fold and by FRAP the difference is 18-fold. The contrast between the two interphase values may be due to systematic errors. Lacking an inverted microscope we were unable to record fluorescence incorporation in interphase cells immediately following microinjection. The manipulations necessary to obtain high space resolution images prevented observation of the more rapid $t_{1/2}s$ and may have disturbed the incorporation process to some extent. The interphase incorporation $t_{1/2}$ we have presented may therefore be an overestimate. On the other hand interphase FRAP $t_{1/2}s$ may be underestimated. Immediately following laser irradiation, there is a rapid partial redistribution of fluorescence that is much faster than mitotic redistributions and not unique to DTAF-tubulin. All fluorescently labeled proteins tested (BSA, ovalbumin, IgG, and tubulin) exhibit this rapid phase. We conclude that it represents the diffusion of fluorescent tubulin dimers not associated with microtubules. It is the subsequent slower redistribution that is likely to represent the exchange of free tubulin dimers with dimers in polymer. It is not possible with our present system of analysis to separate these two phases. Inspection of Fig. 8 will show, however, that the second point following the interphase bleach is substantially above the "best fit" exponential curve. This pattern was common and is likely to result from the free dimer diffusion phase of interphase redistribution. Since all points were used to calculate the "best fit" exponential curves, the mean interphase FRAP $t_{1/2}$ we have presented may be underestimated. Regardless of the difference in interphase incorporation and FRAP $t_{1/2}$ values the two

methods are in agreement that the apparent exchange rate of tubulin between dimer and polymer forms in mitotic cells is more rapid than in interphase cells.

There are substantial variations in apparent exchange rates observed for tubulin within each cell-cycle stage. We identify two possible reasons. First, the $t_{1/2}$ could vary due to the individual characteristics of different cells in the same population. These could include mitotic heterogeneity, as evidenced by the diverse durations of mitosis in cultured cells, and interphase heterogeneity, dependent on whether a cell is in G_1, S or G_2. Second, some variations in $t_{1/2}$ are a result of errors in data processing. Repeated analysis of a single FRAP image series yielded variations in $t_{1/2}$ of as much as 25%. This variation results from human error in the process of measuring relative fluorescence intensities from fluorescence images (30). A significant reduction in error will require a more sophisticated method of data collection and analysis, permitting two-dimensional integration of fluorescence intensities and corrections for photobleaching during observation.

In spite of the large standard deviations, the apparent difference in tubulin dynamics between interphase and mitotic cells is large enough to be highly significant. There are at least two possible sources of the observed difference. One hypothesis is that our apparent rates of tubulin dimer-polymer exchange reflect real rates of exchange. This implies that in addition to differences in organization and apparent function, mitotic and interphase microtubules are also different at a very fundamental level of tubulin behavior. It may be that the relatively dynamic behavior of spindle microtubules reflects a more dynamic behavior of tubulin. Perhaps spindle microtubules require more rapid dimer-polymer dynamics in order to (*a*) rapidly establish a properly organized spindle with the necessary microtubule-kinetochore and microtubule-microtubule interactions and (*b*) respond quickly to the tensile and compressive forces generated during mitosis by the spindle motors. On the other hand, if cytoplasmic interphase microtubules are involved in maintaining cell polarity, shape, and cytoplasmic organization, it may be that a less dynamic tubulin behavior helps maintain these slowly changing properties. A second hypothesis is that the real rate of dimer-polymer exchange is the same in mitosis and interphase but that the number of sites for exchange per unit length of polymer is greater for spindle microtubules than for interphase microtubules. The mechanism and site of subunit exchange have not yet been defined for microtubules in vivo. The site of exchange in vitro has been identified as microtubule ends (2, 5, 14). If they are also the sites of exchange in vivo then a relative abundance of ends in mitotic microtubules could explain the difference in apparent rates of exchange.

Measurements of microtubule length distributions in interphase cells are not available but immunofluorescence images imply that interphase microtubules can be quite long. The fine structure of PTK_1 spindles has been studied with reasonable care (21, 23, 29) but microtubule length distributions have not been reported other than in kinetochore fibers (29). If DTAF-tubulin incorporation and FRAP represent linear incorporation by microtubule treadmilling (20, 45) or by concurrent depolymerization and repolymerization as suggested by the work of Mitchison and Kirschner (24, 25), then a difference in mean microtubule length of between 70- and 18-fold between interphase and mitotic microtubules would be necessary to account for the differences in the rates of exchange that we have observed.

Finally, as suggested by Inoué (11, 13) and Salmon (30, 31) there may be an exchange of tubulin dimers all along the lateral surface of microtubules. In this case length differences should have no effect on observed rates of exchange and our results represent a real difference in mitotic and interphase tubulin dynamics.

We would like to thank Margaret T. Fuller, Susan K. Dutcher, Michael W. Klymkowsky, and R. John Lye for critical reading of this manuscript and Paula M. Grissom for adept technical assistance. This work was supported by grants from the National Institutes of Health (GM31213), the National Science Foundation (PCM-80-14549), and the American Cancer Society (CD8) to J. R. McIntosh. The high voltage electron microscope used is at the national facility in Boulder, Colorado supported by the Biotechnology Resources Program, Division of Research Resources, National Institutes of Health grant # RR-00592.

Received for publication 27 March 1984, and in revised form 16 July 1984.

REFERENCES

1. Anderson, T. F. 1951. Techniques for the preservation of three-dimensional structure in preparing specimens for the EM. *Trans. NY Acad. Sci.* 13:130–134.
2. Bergen, L. G., and G. G. Borisy. 1980. Head to tail polymerization of microtubules *in vitro*. Electron microscope analysis of seeded assembly. *J. Cell Biol.* 84:141–150.
3. Brinkley, B. R., S. M. Cox, D. A. Pepper, L. Wible, S. C. Brenner, and R. L. Pardue. 1981. Tubulin assembly sites and the organization of cytoplasmic microtubules in cultured mammalian cells. *J. Cell Biol.* 90:554–562.
4. Brinkley, B. R., G. M. Fuller, and D. P. Highfield. 1976. Tubulin antibodies as probes for microtubules in dividing and non-dividing cells. *In* Cell Motility. R. Goldman, T. D. Pollard, and J. Rosenbaum, editors. Cold Spring Harbor, New York. pp. 435–456.
5. Bryan, J. 1976. A quantitative analysis of microtubule elongation. *J. Cell Biol.* 71:749–767.
6. DeBrabander, M., R. M. L. Van de Veire, F. E. M. Aerts, M. Borgers, and P. A. J. Janssen. 1976. The effects of [5-(2-thienylcarbonyl)-1H-benzimidazol-2-yl] carbamate, (R 17934; NSC 238159), a new synthetic antitumoral drug interfering with microtubules, on mammalian cells cultured *in vitro*. *Cancer Res.* 36:905–916.
7. DeBrabander, M., G. Geuens, R. Nuydens, R. Willebrords, and J. DeMay. 1981. Taxol induces the assembly of free microtubules in living cells and blocks the organizing capacity of the centrosomes and kinetochores. *Proc. Natl. Acad. Sci. USA.* 78:5608–5612.
8. Giloh, H., and J. W. Sedat. 1982. Fluorescence microscopy: reduced photobleaching of rhodamine and fluorescein protein conjugates by n-propyl galate. *Science* (*Wash. DC*). 217:1252–1255.
9. Graessmann, A., M. Graessman, and C. Mueller. 1980. Microinjection of early SV40 DNA fragments and T antigen. *Methods Enzymol.* 65:816–825.
10. Hiller, G., and K. Weber. 1978. Radioimmunoassay for tubulin: a quantitative comparison of the tubulin content of different established tissue culture cells and tissues. *Cell.* 14:795–804.
11. Inoué, S. 1981. Cell division and the mitotic spindle. *J. Cell Biol.* 91:131s–147s.
12. Inoué, S., J. Fuseler, E. D. Salmon, and G. W. Ellis. 1975. Functional organization of mitotic microtubules. Physical chemistry of the in vivo equilibrium system. *Biophys. J.* 15:725–744.
13. Inoué, S., and H. Sato. 1967. Cell motility by labile association of molecules. *J. Gen. Physiol.* 50:259–292.
14. Karr, T. L., Kristofferson, and D. L. Purich. 1980. Mechanism of microtubule depolymerization. Correlation of rapid induced disassembly experiments with a kinetic model for endwise depolymerization. *J. Biol. Chem.* 255:8560–8566.
15. Keith, C. H., J. R. Feramisco, and M. Shelanski. 1981. Direct visualization of fluorescein-labeled microtubules *in vitro* and in microinjected fibroblasts. *J. Cell Biol.* 88:234–240.
16. Kilmartin, J. V., B. Wright, and C. Milstein. 1982. Rat monoclonal antitubulin antibodies derived by using a new nonsecreting rat cell line. *J. Cell Biol.* 93:576–582.
17. Kreis, T. E., and W. Birchmeier. 1982. Microinjection of fluorescently labeled proteins into living cells with emphasis on cytoskeletal proteins. *Int. Rev. Cytol.* 75:209–227.
18. Kreis, T. E., B. Geiger, and J. Schlessinger. 1982. Mobility of microinjected rhodamine actin within living chicken gizzard cells determined by fluorescence photobleaching recovery. *Cell.* 29:835–845.
19. Leslie, R. J., W. M. Saxton, T. Mitchison, B. Neighbors, E. D. Salmon, and J. R. McIntosh. 1984. Assembly properties of fluorescein labeled tubulin *in vitro* before and after fluorescence photobleaching. *J. Cell Biol.* 99:2146–2156.
20. Margolis, R. L., and L. Wilson. 1978. Opposite end assembly and disassembly of microtubules at steady state *in vitro*. *Cell.* 13:1–8.
21. McDonald, K. L., and U. Euteneuer. 1983. Studies of the structure and organization of microtubule bundles in the interzone of anaphase and telophase PTK_1 cells. *J. Cell Biol.* 97:188*a*. (Abstr.)
22. McIntosh, J. R. 1982. Mitosis and the cytoskeleton. *In* Developmental Order: Its Origins and Regulation, Alan R. Liss, New York. pp. 77–115.
23. McIntosh, J. R., W. Z. Cande, and J. A. Snyder. 1975. Structure and physiology of the mammalian mitotic spindle. *In* Molecules and Cell Movement. S. Inoué and R. E. Stephens, editors. Raven Press, New York. pp. 31–76.
24. Mitchison, T. J., and M. W. Kirschner. 1984. Dynamic instability of microtubule growth. Nature (Lond.). In press.
25. Mitchison, T. J., and M. W. Kirschner. 1984. Microtubule assembly nucleated by isolated centrosomes. *Nature* (*Lond.*). In press.

26. Paweletz, N. 1967. Zur funktion des "Fleming-Koerper" bie der Teilung Tierscher Zellen. *Naturwissenschaften.* 54:533–541.
27. Pickett-Heaps, J. D., D. H. Tippit, and K. R. Porter. 1982. Rethinking mitosis. *Cell.* 29:729–744.
28. Porter, K. R. 1966. Cytoplasmic microtubules and their functions. *CIBA Found. Symp.* pp. 308–356.
29. Rieder, C. L. 1981. The structure of the cold stable kinetochore fiber in metaphase PTK_1 cells. *Chromosoma.* 84:145–158.
30. Salmon, E. D., R. J. Leslie, W. M. Saxton, M. L. Karow, and J. R. McIntosh. 1984. Spindle microtubule dynamics in sea urchin embryos. *J. Cell Biol.* 99:2165–2174.
31. Salmon, E. D., M. McKeel, and T. Hays. 1984. The rapid rate of tubulin dissociation from microtubules in the mitotic spindle in vivo measured by blocking polymerization with colchicine. *J. Cell Biol.* 99:1064–1075.
32. Salmon, E. D., W. M. Saxton, R. J. Leslie, M. L. Karow, and J. R. McIntosh. 1984. Diffusion coefficient of fluorescein-labeled tubulin in the cytoplasm of embryonic cells of a sea urchin. *J. Cell Biol.* 99:2157–2164.
33. Stacey, D. W., and V. G. Allfrey. 1977. Evidence for the autophagy of microinjected proteins in HeLa cells. *J. Cell Biol.* 75:807–817.
34. Taylor, D. L., P. A. Amato, K. Luby-Phelps, and P. McNeil. 1984. Fluorescent analog cytochemistry. *Trends in Biochem. Sci.* 9:88–91.
35. Taylor, D. L., and Y. L. Wang. 1978. Molecular cytochemistry: Incorporation of fluorescently labeled actin into living cells. *Proc. Natl. Acad. Sci. USA.* 75:857–861.
36. Taylor, D. L., and Y.-L. Wang. 1980. Fluorescently labeled molecules as probes of the structure and function of living cells. *Nature (Lond.).* 284:405–410.
37. Tucker, J. B. 1979. Spatial organization of microtubules. *In Microtubules.* K. Roberts and J. S. Hyams, editors. Academic Press, London. pp. 315–357.
38. Wadsworth, P., and R. D. Sloboda. 1983. Microinjection of fluorescent tubulin into dividing sea urchin cells. *J. Cell Biol.* 97:1249–1254.
39. Wadsworth, P., and R. D. Sloboda. 1984. Modification of tubulin with the fluorochrome 5-(4,6-Dichlorotriazyn-2-yl) amino fluorescein and the interaction of the fluorescent protein with the isolated meiotic apparatus. *Biol. Bull.* 166:357–367.
40. Wang, K., J. R. Feramisco, and J. F. Ash. 1982. Fluorescent localization of contractile proteins in tissue culture cells. *Methods Enzymol.* 85:514–562.
41. Wang, Y.-L., J. M. Heiple, and D. L. Taylor. 1982. Fluorescent analog cytochemistry of contractile proteins. *In* Methods in Cell Biology L. Wilson, editor. Academic Press, Inc. New York. 25:1–11.
42. Wang, Y.-L., and D. L. Taylor. 1980. Preparation and characterization of a new molecular cytochemical probe: 5-iodoacetamidofluorescein-labeled actin. *J. Histochem. Cytochem.* 28:1198–1206
43. Webb, W. W., L. S. Barak, D. W. Tank, and E.-S. Wu. 1980. Molecular mobility on the cell surface. *Biochem Soc. Symp.* 46:191–205.
44. Weber, K., and M. Osborn. 1979. Intracellular display of microtubule structures revealed by indirect immunofluorescence microscopy. *In* Microtubules. K. Roberts and J. S. Hyams, editors. Academic Press, Inc., London. pp. 279–313.
45. Wegner, A. 1976. Head to tail polymerization of actin. *J. Mol. Biol.* 108:139–150.
46. Zavortink, M., M. J. Welsh, and J. R. McIntosh. 1983. The distribution of calmodulin in living mitotic cells. *Exp. Cell Res.* 149:375–385.
47. Zieve, G. W., D. Turnbull, J. M. Mullins, and J. R. McIntosh. 1980. Production of large numbers of mitotic mammalian cells by use of the reversible microtubule inhibitor Nocodazole. *Exp. Cell Res.* 126:397–405.